

The nature of [N–Cl–N]⁺ and [N–F–N]⁺ halogen bonds in solution†

Cite this: *Chem. Sci.*, 2014, 5, 3226

Alavi Karim, Marcus Reitti, Anna-Carin C. Carlsson, Jürgen Gräfenstein and Máté Erdélyi*

Halonium ions are synthetically useful, transient species that may be stabilized by attachment to two electron donors. Whereas studies of [C–X–C]⁺-type ions have greatly contributed to the fundamental understanding of chemical bonding and reaction mechanisms, investigations of the corresponding [N–X–N]⁺ halogen bond complexes are only at an early stage. Herein we present solution NMR spectroscopic and theoretical evidence for the nature of [N–Cl–N]⁺ and [N–F–N]⁺ complexes, and we discuss their geometries and stabilities in comparison to their iodine and bromine-centered analogues as well as the corresponding three-center [N–H–N]⁺ hydrogen bond. We show the chlorine-centered halogen bond to be weaker but yet to resemble the symmetric geometry of the three-center bond of heavier halogens. In contrast, the [N–F–N]⁺ bond is demonstrated to prefer asymmetric geometry analogous to the [N–H–N]⁺ hydrogen bond. However, the [N–F–N]⁺ system has a high energy barrier for interconversion, and due to entropy loss, its formation is slightly endothermic.

Received 22nd April 2014

Accepted 27th May 2014

DOI: 10.1039/c4sc01175a

www.rsc.org/chemicalscience

Introduction

Following the initial discussions of Noyes¹ and Stieglitz,² the existence of halonium ions as reactive intermediates was first postulated in the mechanistic investigations of electrophilic addition of halogens to alkenes.³ Over the past century, halonium ions have gained wide utility in organic chemistry, providing access to organohalides of vast synthetic impact, for example, in the material and pharmaceutical sciences. Studies of these species have yielded valuable insights into the basic rules governing the mechanisms of their chemical transformations.⁴ Being transient species, 'naked' electrophilic halogens lack prolonged lifetime and are therefore typically studied as part of three-center systems commonly stabilized by attachment to two carbon atoms. These molecular systems may adopt linear or triangular geometries. Since their description by Olah *et al.*,⁵ the solution structure of halonium ions has been heavily debated with spectroscopic and computational evidence provided both for and against the static symmetric [C⋯X⋯C]⁺ geometry and the corresponding rapidly interconverting pair of asymmetric [C–X⋯C]⁺ ⇌ [C⋯X–C]⁺ arrangements.^{6–8} Whereas the former geometry is proposed to be stabilized by the covalent character of its two identically long and strong C⋯X bonds, the latter is commonly referred to as a resonance-stabilized arrangement. In addition to the comparably well-studied

[C–I–C]⁺ and [C–Br–C]⁺ ions, the first investigations of the analogous chlorine and fluorine-centered systems were reported only very recently.^{9,10}

Stabilization of halonium ions by attachment to two nitrogen atoms, instead of carbons, is as challenging as it is impactful. The properties of iodine and bromine-centered [N–X–N]⁺ bonds stabilized by two identical nitrogenous electron donors were evaluated by X-ray,¹¹ IR,¹² solution NMR and *in silico* techniques.^{13–16} They possess linear structures with two equivalent N⋯Br or N⋯I secondary bonds in both the solid state and in solution.^{12,13} These halogen bonds^{17–19} are unusually strong and have, in addition to electrostatic, substantial covalent character.^{13,14,20} The analogous [N–H–N]⁺ three-center hydrogen bonds have been described as asymmetric in solution yet symmetric in the solid state,¹⁹ although a contradictory opinion has also been expressed.²¹ These bonds lack great strength.²² Thus far, the symmetry and the strength of [N–X–N]⁺ and [N–H–N]⁺ bonds are two of the few significant differences found between the nature of hydrogen and halogen bonds, commonly reported as fundamentally similar interactions.^{23,24}

The three-center [N–I–N]⁺ complex, bis(pyridine)iodonium tetrafluoroborate, has found applications in synthetic organic chemistry as an electrophilic halogenation, cross-coupling, and oxidizing agent.²⁵ Along with its bromine centered analogue, it has also been studied for the development of chiral halonium transfer agents.²⁶ Comparable [N–Cl–N]⁺ species, with the much more reactive Cl⁺ stabilized by two nitrogen donors, have so far not been detected in solution but have only been evidenced by mass spectrometry as short lived species in the gas phase.^{27,28} The structure of the [N–Cl–N]⁺ species along with that of the

Department of Chemistry and Molecular Biology, University of Gothenburg, SE-412 96 Gothenburg, Sweden. E-mail: mate@chem.gu.se; Tel: +46-31-786 9033

† Electronic supplementary information (ESI) available: Details on the synthesis, spectroscopic data for compound identification, and details on the NMR and computational symmetry investigations. See DOI: 10.1039/c4sc01175a

analogous $[\text{N-F-N}]^+$ system was computationally predicted by one group to be symmetric with two equal N-Cl or N-F bonds,²⁹ whereas other workers have reported the $[\text{N-Cl-N}]^+$ complex to be symmetric but the $[\text{N-F-N}]^+$ analogue to be asymmetric,¹⁶ *i.e.* encompassing a distinct covalent N-F bond and another longer, weaker $\text{N}\cdots\text{F}$ halogen bond. The $[\text{N-Cl-N}]$ bond was predicted to be asymmetric by Parra.¹⁵ So far no experimental evidence of the symmetry or asymmetry of these bonds is available. Such electrophilic species are of considerable theoretical interest, and upon careful optimization may gain practical importance.^{3,25} The halogen bond is anticipated to develop into a molecular tool complementary to the hydrogen bond for rational modulation of molecular recognition processes,²⁴ with direct applicability in crystal engineering³⁰ and drug design.³¹ This potential gives the understanding of the properties of the halogen bonds, including the more difficult to investigate chlorine and fluorine-centered bonds, critical importance. Three-center halogen bonds are of particular interest because of their unusual strength.^{13,19,24} Solution studies of halogen bonds are still scanty.^{17,32-34} Herein, we present the study of chlorine and fluorine-centered halogen bonded systems by a combination of solution NMR and computational methods, and we discuss their properties in comparison to their iodine and bromine-centered analogues as well as to the three-centered hydrogen bond.

Results and discussion

Synthesis

The bis(pyridine)halonium triflate complex was demonstrated to be a suitable model system for solution investigation of the iodine **1** and bromine **2** centered $[\text{N-X-N}]^+$ halogen bonds,^{13,14} and was therefore employed for the exploration of the chlorine **3** and fluorine-centered **4** analogues. For preparation of **3**, we have modified the previously developed³⁵ synthetic route to **1** and **2**. Bis(pyridine)silver(I) triflate, which had been generated in advance and thoroughly dried under vacuum, was dissolved in dry CD_2Cl_2 solution and treated with Cl_2 gas while being kept at -80°C and agitated by ultrasonication for 30 minutes (ESI Fig. S1†). The mixture was then centrifuged to remove silver chloride precipitate prior to transferring the bis(pyridine)chloronium triflate **3** solution through a precooled, dry cannula into a precooled, dry NMR tube fitted with a septum, which was then immediately transferred into the NMR magnet. Throughout the entire process, the solution was carefully kept moisture-free under an argon atmosphere and at -80°C to avoid decomposition, which is readily noticeable by the disappearance of the yellow color of the $[\text{N-Cl-N}]^+$ complex **3**. Because of known difficulties associated with the use of F_2 gas,³⁶ we have not followed the above synthetic route for the generation of the corresponding $[\text{N-F-N}]^+$ complex **4**. Instead, we prepared it by mixing a CD_3CN solution of *N*-fluoropyridinium tetrafluoroborate **8** with pyridine **9** at -35°C . This solution was stable at low temperature for several days, but gave a complex mixture at room temperature, in line with the high reactivity of electrophilic fluorine. Low CD_2Cl_2 solubility of **8** motivated the selection of CD_3CN as solvent. DFT calculations predict

comparable geometry for **4** in CD_2Cl_2 and in CD_3CN (ESI†). The $[\text{N-X-N}]^+$ bonds of **1** and **2** were previously shown to be unaffected by changing the solvent from CD_2Cl_2 to CD_3CN .¹⁴

NMR

The formation of the bis(pyridine)chloronium triflate **3** complex caused a considerable deshielding of the ^1H and ^{13}C NMR shifts of pyridine **9** (Table 1). In addition to the increased chemical shifts, formation of **3** was indicated by the enhanced relaxation rate of the atoms close to the quadrupolar chloronium nucleus. The longitudinal relaxation time (T_1) of the pyridine H-2 protons decreased from 1.5 s in bis(pyridine)silver(I) triflate, the synthetic intermediate from which it was prepared, to 0.08 s in compound **3** (Fig. 1). This rapid relaxation, along with the limited lifetime ($t_{1/2} \sim 10\text{--}12$ hours) of **3** even at -80°C , prevented detection of the chemical shift of the pyridine nitrogen in the $[\text{N-Cl-N}]^+$ complex. Upon increase in temperature, rapid decomposition of **3** was observed, which prevented us from measuring the temperature dependence of deuterium equilibrium isotope effects of **3**, in accordance with that previously reported for **1** and **2**¹³ for spectroscopic investigation of its symmetry. Thus, for **3** no experimental distinction between a static symmetric and a pair of rapidly interconverting asymmetric structures was possible. In contrast to its iodine, bromine and chlorine-centered analogues, **1-3**, pyridine *N*-fluoropyridinium tetrafluoroborate **4** gave two sets of ^1H , ^{13}C and ^{15}N NMR signals (Fig. 2 and Table 1), indicating that its pyridines are in different chemical environments. One set, *i.e.* δ_{H} 9.22, 8.65 and 8.23 ppm, shows $^1\text{H}\text{--}^{19}\text{F}$ scalar couplings, as confirmed by ^{19}F -decoupled ^1H NMR spectra, indicating a strong N-F covalent bond. In agreement with the literature on related compounds,³⁷ the corresponding ^{19}F NMR signal at 45.9 ppm is broadened by multiple-bond proton-fluorine couplings. This bonding pattern was further confirmed by ^1H decoupled ^{19}F NMR. The ^1H , ^{13}C , ^{15}N and ^{19}F chemical shifts for the more strongly bonded pyridine ring compare well to those of *N*-fluoropyridinium tetrafluoroborate **8** (Table 1 and Fig. S17–S21†). The second set of pyridine signals of **4** at δ_{H} 8.55, 7.75 and 7.34 ppm do not show $^1\text{H}\text{--}^{19}\text{F}$ couplings. Its ^1H , ^{13}C and ^{15}N NMR chemical shifts (Table 1) are similar to but slightly different from those of pyridine **9**. The translational diffusion rate of this ring ($D(^1\text{H}) = 46.7 \times 10^{-10} \text{ m}^2 \text{ s}^{-1}$) is significantly higher than those of the *N*-fluorinated pyridine ($D(^1\text{H}) = 41.2 \times 10^{-10} \text{ m}^2 \text{ s}^{-1}$) and of the tetrafluoroborate counter ion ($D(^{19}\text{F}) = 41.3 \times 10^{-10} \text{ m}^2 \text{ s}^{-1}$). At the same temperature (-35°C) and in the same solvent (CD_3CN), *N*-fluoropyridinium tetrafluoroborate **8** diffuses considerably faster ($D(^1\text{H}) = D(^{19}\text{F}) = 120.3 \times 10^{-10} \text{ m}^2 \text{ s}^{-1}$) in the absence of pyridine **9**. Neither NOE between the protons of the two pyridines of **4**, nor HOE between the fluorine of *N*-fluoropyridinium ion and the hydrogens of the weakly coordinated pyridine was observed. The above data are most compatible with a weakly interacting mixture of pyridine **9** and *N*-fluoropyridinium tetrafluoroborate **8**. Whereas the diffusion data indicates independently moving pyridine rings for **4**, its slight chemical shift differences from **8** and **9** suggest very weak coordination. The magnitude of ^{15}N NMR shift alteration

Table 1 Observed NMR chemical shifts of the studied pyridine complexes

Substance	#	X	C.I.	Temp	Chemical shift (ppm)							
					H2	H3	H4	C2	C3	C4	N	F
	1	I	OTf ⁻	25 °C	8.79	7.64	8.23	150.6	128.3	142.7	-175.1	
	2	Br	OTf ⁻	25 °C	8.74	7.76	8.24	146.9	128.2	142.7	-142.9	
	3	Cl	OTf ⁻	-80 °C	8.87	8.02	8.46	145.7	129.4	144.8	n.d.	
	4	F	BF ₄ ⁻	-35 °C	9.22 8.55	8.23 7.34	8.65 7.75	137.1 150.2	130.8 124.7	147.4 137.1	-122.1 -68.8	45.9
	8	F	BF ₄ ⁻	25 °C	9.19	8.26	8.68	137.2	131.3	148.1	-122.1 ^a	47.0
	9	—		25 °C	8.76	7.68	8.13	145.4	126.2	142.0	-65.8 ^a	
	10	F	B ₂ F ₇ ⁻	25 °C	9.17 8.71	8.25 8.06	8.67 8.62	137.2 142.6	131.3 128.7	148.9 148.1	-123.6 -185.3	45.7

^a Data given for -35 °C for comparability, C.I., counter ion; n.d., not determined.

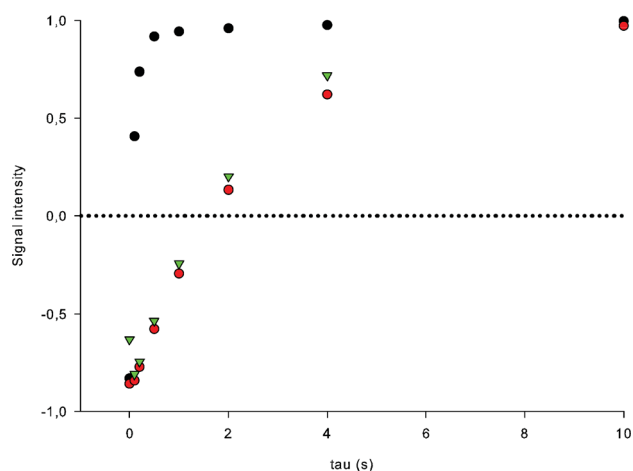


Fig. 1 The longitudinal spin-lattice (T_1) relaxation rate of H-2 as measured by inversion-recovery experiment at -80 °C in CD_2Cl_2 solution and visualized by plotting signal intensity vs. time. The data points of bis(pyridine)chloronium triflate **3** are in black ($T_1 = 0.08$ s), those of bis(pyridine)silver(I) triflate in green ($T_1 = 1.49$ s), whereas those of pyridine **9** in red ($T_1 = 1.61$ s). The exceptionally rapid relaxation observed for **3** is the consequence of the quadrupolar moment of chlorine(I).

observed upon mixing **8** and **9** (-3 ppm, Table 1 and Fig. S23†) better compares to that observed for conventional two-center halogen bonds³⁸ rather than three-center bonds of the heavier halogens.¹³

We have also studied the commercially available pyridine *N*-fluoropyridinium heptafluorodiborate **10** complex that gives a stable CD_2Cl_2 solution at room temperature. Similar to **4**, compound **10** shows two sets of NMR signals (Fig. S10–S16†). One of its pyridine rings possesses 1H - ^{19}F couplings as well as chemical shifts comparable to that of the *N*-fluoropyridinium tetrafluoroborate **8** (Fig. S17–S21†) and of the *N*-fluorinated pyridine of **4** (Fig. S4–S9† and Table 1). The second ring shows

chemical shifts that are dissimilar to pyridine **9**, with the most significant difference detected for its ^{15}N chemical shift (-185.3 vs. -67 ppm,¹³ 25 °C). In addition, significantly broadened 1H NMR signals as compared to those of **4** and an additional broad signal at 13.1 ppm (Fig. S15†) were detected for this ring, which are incompatible with its proposed pyridine *N*-fluoropyridinium heptafluorodiborate structure.³⁹ Its -185.3 ppm ^{15}N NMR chemical shift better compares to that of *N*-methylpyridinium iodide ($\delta_{15N} = -180.5$ ppm)¹³ and of protonated pyridinium triflate ($\delta_{15N} = -186.5$ ppm) than to the chemical shift of free pyridine ($\delta_{15N} = -67$ ppm).¹³ These data along with the comparable translational diffusion rates for the two pyridines of **10** (16.9×10^{-10} vs. 16.6×10^{-10} m² s⁻¹, CD_2Cl_2 , 25 °C) suggest that the nitrogen of this pyridine is quaternalized, likely with a substituent of comparable size to fluorine. Direct interaction of the nitrogen of this pyridine with the $B_2F_7^-$ counter ion is not supported by the similar ^{11}B and ^{19}F NMR shifts of **8** ($\delta_B -1.2$ ppm, $\delta_F -151.7$ ppm) and **10** ($\delta_B -1.1$ ppm, $\delta_F -150.7$ ppm). Thus, this pyridine of **10** is likely protonated and is thereby turned into a weaker nucleophile than pyridine itself, explaining the stability of the CD_3CN solution of pyridine *N*-fluoropyridinium heptafluorodiborate **10** at room temperature in contrast to the rapid reaction observed upon addition of pyridine **9** to *N*-fluoropyridinium tetrafluoroborate **4** at the same temperature. Addition of pyridine to the solution of **10** yielded a complex product mixture.

The above observations support the structure *N*-fluoropyridinium pyridinium tetrafluoroborate trifluorohydroxyborate [$C_5H_5N^+ - F][C_5H_5NH^+][BF_4^-][BF_3(OH)^-]$ for **10**, proposed by Banks, *et al.*,⁴⁰ but not previously proven.

Computational studies

In order to gain further insight into the nature of the halogen bonds of complexes **3** and **4**, we studied their geometric stability computationally. To keep this study comparable to the previous

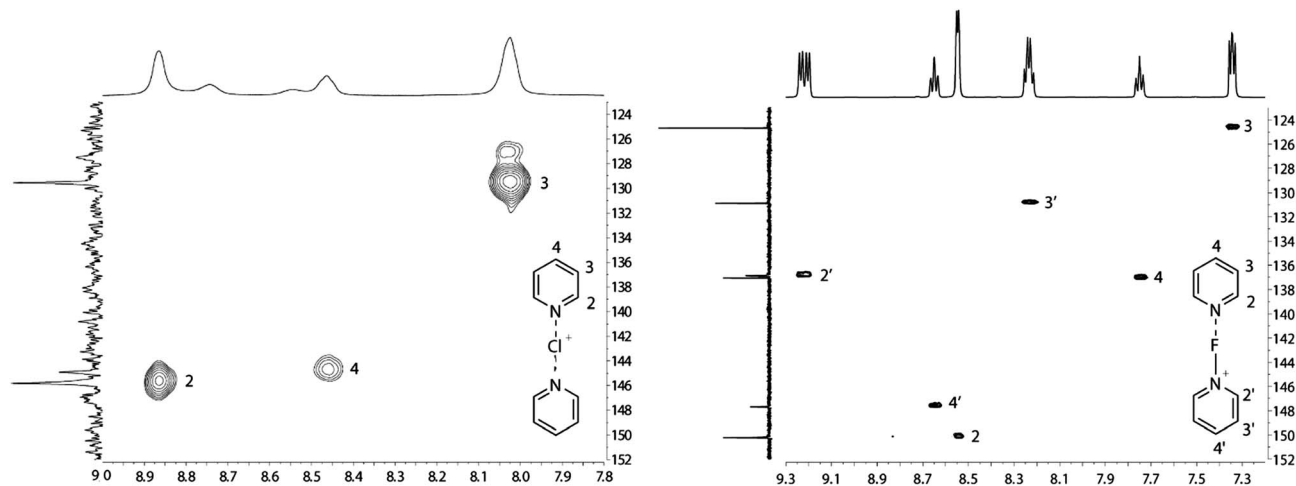


Fig. 2 The ^1H , ^{13}C HSQC spectra of bis(pyridine)chloronium triflate **3** (CD_2Cl_2 , -80°C) and of pyridine *N*-fluoropyridinium tetrafluoroborate **4** (CD_3CN , -35°C). Due to rapid relaxation, the cross peaks of **3**, to the left, are severely broadened. Its ^1H NMR spectrum also shows the signals of bis(pyridine)protonium triflate, which is formed upon moisture-induced decomposition. For **4**, to the right, two sets of pyridine signals are seen: one shows distinct ^1H - ^{19}F couplings whereas the second does not.

investigations of closely related compounds (**1** and **2**)^{13,14,35} calculations were performed with density-functional theory using the B3LYP functional.^{41–45} The LANL08d basis set⁴⁶ in conjunction with the LANL2DZ effective core potential (ECP)^{47–49} was used for I and Br, Pople's 6-311+G(d,p) basis sets^{50–52} for N, F and Cl and Pople's 6-311G(d,p) basis sets^{50,51} for the remaining atoms. This construction of the basis set ensures that the basis set (i) is of triple-zeta quality including polarization functions for all atoms, (ii) provides diffuse functions for all atoms involved in halogen bonds, and at the same time, keeps the size of the basis set still tractable. Equilibrium geometries were calculated and characterized in CH_2Cl_2 ($\epsilon = 8.93$) using the polarizable continuum model (PCM).^{53,54} Selected geometries were reoptimized for CH_3CN solution ($\epsilon = 35.69$). The surfaces of the solvent cavities were constructed as solvent-excluded surfaces using the united-atom topological model (Gaussian09 keywords *Surface = SES, Radii = UA0*). For the potential energy surface scans the geometry of the complexes were held in a planar arrangement with regard to the two pyridines. The electrostatic potential maps were generated using Spartan⁵⁵ and were computed on the 0.001 au contour of the electron density. All calculations were performed with the Gaussian09 package.⁵⁶

A DFT description of the three-center four-electron (3c4e) bonds in the $[\text{N-X-N}]^+$ complexes is subtle due to the incomplete description of non-dynamic electron correlations in these bonds on the one hand,⁵⁷ and the self-interaction error inherent to DFT on the other hand.⁵⁸ In earlier work by our group, B3LYP has been assessed against second order Møller-Plesset (MP2) perturbation theory⁵⁹ and been proven to be a suitable model for these types of complexes. In addition, we have performed test calculations for **3**, **7**, and pyridine with MP2 as well as the M06-2X functional⁶⁰ and B3LYP-D3, *i.e.* B3LYP complemented with Grimme's dispersion corrections.⁶¹ The results for the N-X bond lengths and the thermochemical data (see ESI[†]) confirm that B3LYP with the triple-zeta basis set described above

provides a reliable description of the complexes **1–4**. This finding is in line with ref. 16, where CCSD(T) calculations were found to yield geometries and energies comparable to those from DFT. At this point, it has to be noted that the description of the $[\text{N-X-N}]^+$ bonds is rather challenging, and even advanced methods (*e.g.* CCSD(T) and CCSD) may provide energies differing by more than 15 kJ mol^{-1} for a given reaction.¹⁶ In particular, the reference computations demonstrated that the partial ionic character makes the charged halogen bonds investigated here unusually short and strong^{13,14,16,35,62} so that the contribution of dispersion interactions to the overall attraction is just a small correction, in contrast to neutral halogen bonds for which these play a pivotal role. The effect of the basis-set superposition error (BSSE) for 3c4e halogen bond was earlier proven negligible.³⁵

The $[\text{N-Cl-N}]^+$ complex **3**, similar to its iodine and bromine centered analogues **1** and **2**,^{13,14,35} was predicted to be symmetric (Fig. 3). Computed frequencies for the stretching vibrations, given in Table 2, are consistent with the proposed structures. The calculated frequency for the asymmetric N-X-N stretching vibration in **3** depends on the computation method quite sensitively, varying between 90 cm^{-1} for M06-2X and 212 cm^{-1} for MP2. This reflects the fact that this vibration probes both the orbital delocalization and the charge transfer in the $[\text{N-X-N}]^+$ moiety. However, all methods used consistently predict a symmetric structure for **3**. The calculated frequencies for the symmetric N-X-N stretching vibration in **3** are, in contrast, within the narrow interval between 173 cm^{-1} (B3LYP-D3) and 190 cm^{-1} (M06-2X). The calculated N-Cl distance is 0.3 \AA longer than the corresponding N-Cl covalent bond (1.726 \AA , Table 2) of the hypothetical *N*-chloropyridinium complex **7**, and 1.3 \AA shorter than the sum of the van der Waals radii⁶³ of the involved atoms (1.55 \AA (N) + 1.75 \AA (Cl) = 3.3 \AA). It should be noted that the bond shortening relative to the sum of the van der Waals radii of the nitrogen and the involved halogen is 39% for **3** (Cl)

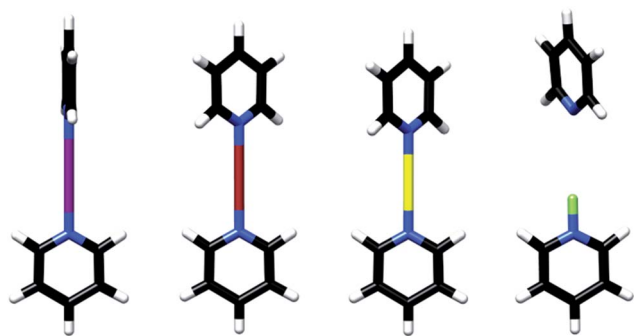
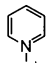


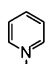
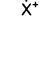


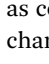
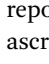
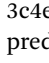
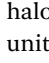


Fig. 3 DFT geometry optimization (B3LYP/LANL08d) predicted static, symmetric $[N-X-N]^+$ halogen bonds for the iodine, bromine and chlorine-centred bis(pyridine)halonium complexes 1–3, shown from the left to the right, whereas an asymmetric arrangement for the fluorine-centred 4. Iodine is shown in violet, bromine in red, chlorine in yellow and fluorine in green. The nitrogen–nitrogen, and nitrogen–halogen distances of 1–4 are given in Table 2.

Table 2 Computationally predicted N–X and N–N distances [Å], and stretching vibration frequencies $[cm^{-1}]$ for the equilibrium geometries of the bis(pyridine)halonium complexes 1–4 and the corresponding *N*-halopyridinium 5–8. Computations done with B3LYP and with CH_2Cl_2 solvent model, unless otherwise stated

#, X	d_{N1-X}	d_{N2-X}	d_{N-N}	ν_{N-X}	ν_{N-X-N}	
					ν_{symm}	ν_{asymm}
 1, I	2.303	2.303	4.604	166	167	
 2, Br	2.140	2.140	4.280	173	165	
 3, Cl	2.025	2.025	4.050	175	123	
 3, Cl ^a	2.025	2.025	4.050	—	173	121
 3, Cl ^b	1.994	1.994	3.988	185	212	
 3, Cl ^c	1.982	1.982	3.964	190	90	
 4, F	1.360	3.499	4.860	32	536	
 5, I	2.093	—	—	260	—	—
 6, Br	1.893	—	—	318	—	—
 7, Cl	1.726	—	—	428	—	—
 8, F	1.360	—	—	534	—	—

^a B3LYP-D3. ^b MP2. ^c M06-2X.

as compared to 37% for 2 (Br) and 35% for 1 (I). These relative changes are significantly larger than the <30% shortening reported for conventional halogen bonds^{19,24,64} and may be ascribed to the covalent character of the $N\cdots X$ halogen bonds of 3c4e systems.^{65,66} Natural population analysis⁶⁷ (Table S4†) predicts increasing charge delocalization with decreasing halogen size of $[N-X-N]^+$ complexes: -0.59 , -0.72 and -0.84 unit charges are transferred to the pyridine rings in 1, 2 and 3, respectively.

For a more comprehensive picture of the stability of 1–4, relaxed potential energy surface (PES) calculations were performed by varying the distance between the pyridine N atoms from 3.2 to 8.0 Å with 0.1 Å increments and N–X distances between 3.2 Å and 8.0 Å with 0.1 Å increments. In agreement with the geometry optimization, for 1–3 a single energy minimum was detected confirming the preference of

three-center systems for a static, symmetric geometry (Fig. 4). Accordingly, the predicted potential energy surface of 4 shows two equal global energy minima at N–F distances consistent with two comparable asymmetric geometries that are separated by a 151.0 kJ mol^{-1} energy barrier, making their interconversion, as described for the corresponding tautomerizing $[N-H\cdots N]^+$ complex,^{13,35,68} unlikely. Formation of bis(pyridine) fluoronium complex 4 is endothermic with $\Delta G = 21.3\text{ kJ mol}^{-1}$ due to the loss of entropy ($\Delta E = -2.7\text{ kJ mol}^{-1}$). That is, at room temperature 4 is predicted to prevail as a mixture of uncoordinated *N*-fluoropyridinium ion 8, possessing a covalent N–F bond, and non-complexed pyridine 9. In contrast, the formation of the corresponding halogen bonded complexes 1–3 from pyridine and *N*-halopyridinium ions 5–7 provide free energy gains of 58.6 (1), 42.7 (2) and 9.5 kJ mol^{-1} (3), (Table S1†), the energy gains being 109.2 (1), 92.9 (2) and 57.5 (3) kJ mol^{-1} , respectively. The overall energy change upon formation of these 3c4e bonds also includes the energy requirement for stretching the N–X covalent bond of 5–7 to the bond length of the corresponding symmetric complexes 1–3 (Table S2†). With the estimated 22.3 kJ mol^{-1} stretching energy for iodine (2.093 Å in 5 to 2.303 Å in 1), 35.6 kJ mol^{-1} for bromine (1.893 Å in 6 to 2.140 Å in 2), and 57.9 kJ mol^{-1} for chlorine (1.726 Å in 7 to 2.027 Å in 3), the gross energy gain upon bond formation is ~ 110 – 130 kJ mol^{-1} . These values are amazingly large energies for formation of halogen bonds. The symmetric $[N\cdots X\cdots N]^+$ 3c4e complexes of 1–3 are predicted to be 16 – 20 kJ mol^{-1} more stable than the corresponding asymmetric $[N-X\cdots N]^+$ complexes encompassing conventional covalent and halogen bonds (Table S3†). Conversely, creation of a symmetric $[N-F-N]^+$ bond, on the saddle point of the double well in Fig. 3, would require 140.7 kJ mol^{-1} stretching energy (1.360 Å in 8 to 1.800 Å) and an overall 138 kJ mol^{-1} energy investment (Tables S2 and S3†). Accordingly, 4 does not form a symmetric complex.

In line with previous observations, the magnitudes of the σ -hole of the halogens of 5–8 (Fig. 4) follow the order of $I > Br > Cl \gg F$, with that of the fluorine of 8 predicted to teeter at the edge of existence. This trend suggests that the $[N-X-N]^+$ bond has a stronger ionic character the heavier the halogen atom is. This suggestion is supported by other observations: (i) as mentioned above, the total transfer of electron charge into the halogen increases in the order $I < Br < Cl$. This charge transfer both accounts for covalent bonding and decreases the electrostatic attraction between the halonium ion and the pyridine rings. (ii) The same trend, albeit less distinct, is observed for the charge transfer to the halogen when 1 to 3 are formed from 5 to 7, respectively (see Table S4†): this charge transfer amounts to -0.10 , -0.11 , and -0.12 for I, Br, and Cl, respectively. (iii) A second-order perturbation theory analysis of the Fock matrix in natural bond orbitals (NBO)⁶⁹ for 1 to 3 reveals that the delocalization from the N lone-pair orbitals into the N–X $p\sigma^*$ bond orbital is the leading contribution to the stabilization of the halogen bond. The NBO second-order energy for this interaction amounts to 454 , 628 , and 808 kJ mol^{-1} , respectively, for 1 to 3 (see Table S5†). This decrease of the interaction energy with increasing atomic number of the halogen is caused by (i) an increase of the Fock matrix element between the two NBOs and

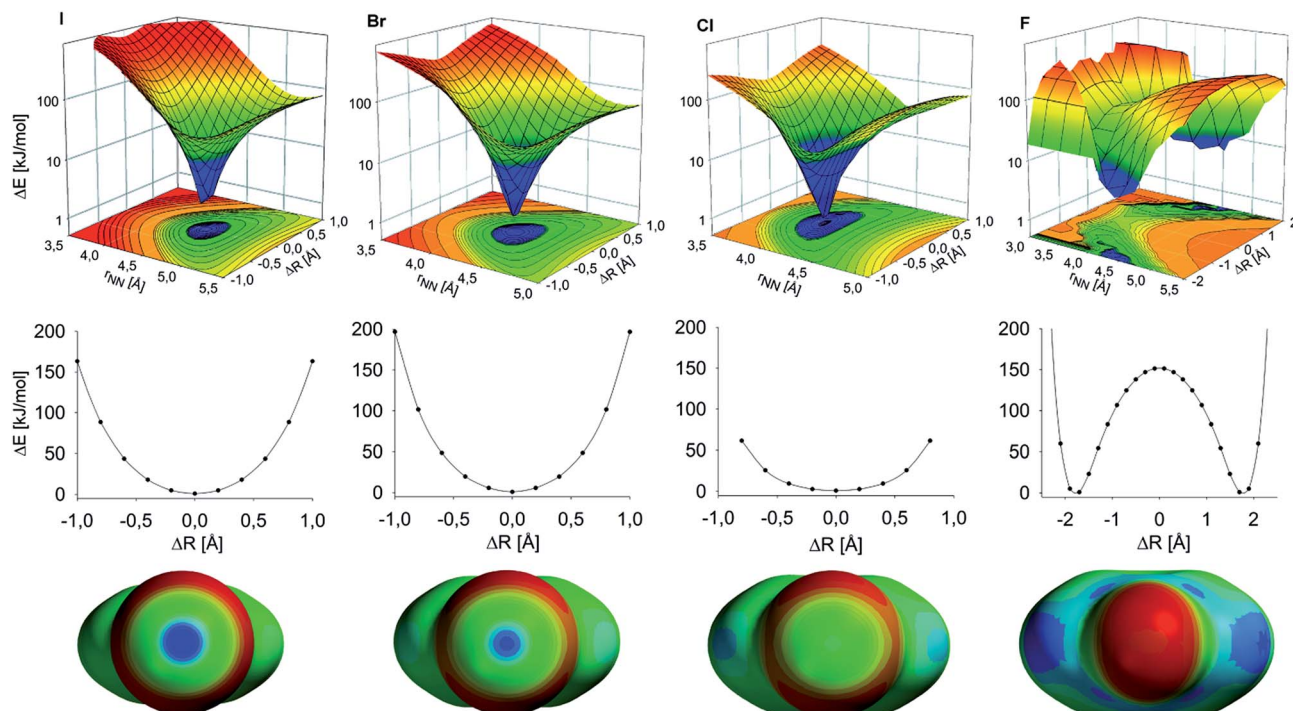


Fig. 4 The computed potential energy surface of bis(pyridine)halonium complexes describes the relationship between their geometry and energy. *Upper row*: the potential energy as a function of the nitrogen–nitrogen, r_{NN} , and the N–X distance is shown, where ΔR is the difference between the $\text{N}_1\text{--X}$ and $\text{N}_2\text{--X}$ distances at a given r_{NN} . The potential energy surfaces describing the halogen motion for the bis(pyridine)iodonium **1**, bromonium **2** and chloronium **3** complexes, from the left to the right, possess a single energy minimum reflecting a static, symmetric geometry whereas that of the fluoronium complex **4** shows two equal minima revealing its preference for an asymmetric arrangement. *Middle row*: the 2D-slices corresponding to the N–N distance with the global energy minimum of each complex is shown. *Bottom row*: the surface electrostatic potential of the halogen of **5–8** are shown visualizing the sigma hole I, Br, Cl and F corresponding to 531.8, 508.4, 464.0, and 343.4 kJ mol^{-1} , respectively. The surface was computed on the 0.001 au contour of the electronic density. Color ranges, in kJ mol^{-1} , are as follows: red, less than 350, yellow between 350 and 390, green between 390 and 470, light blue between 470 and 490, and blue greater than 490.

(ii) a decrease of the energy for the N–X bond orbital from **1** to **3** (see Table S5[†] for details). Altogether, our investigations support the conclusions in ref. 16 that the $[\text{N--X--N}]^+$ bond more resembles a covalent bond for light halogen atoms but a dative bond for heavy halogens.

Conclusions

We present the first experimental evidence for stabilization of a chloronium ion in solution by attaching it to two nitrogens. The chlorine centered 3c4e halogen bond prefers a static symmetric geometry, analogous to that of the heavier halogens.¹³ The corresponding fluorine centered 3c4e halogen bonded system adopts an asymmetric structure, similar to the analogous $[\text{N--H}\cdots\text{N}]^+$ hydrogen bond. However, in contrast, its interconversion, $[\text{N--F}\cdots\text{N}]^+ \rightleftharpoons [\text{N}\cdots\text{F--N}]^+$, is hindered by a high energy barrier. Its formation is thermodynamically disfavored, in line with fluorine being a poor halogen bond donor.^{23,24,70,71}

The bonding of **1–4** resembles the transition state structure of an $\text{S}_{\text{N}}2$ reaction,^{72,73} one of the most important transformations in organic chemistry. Thus, the linear arrangement of the nucleophile, the central carbon atom and the leaving group along with the number of electrons intimately involved in an $\text{S}_{\text{N}}2$ reaction correspond to that of three-center-four electron

species.^{73,74} While the symmetric, linear geometry is the global energy minimum for **1–3**, it is a high-energy transition state for the $\text{S}_{\text{N}}2$ reaction and for **4**. The nature of 3c4e systems remains an unsolved enigma.⁷⁴ Model systems such as **1–4** provide valuable insights into the fundamentals of reaction and chemical bonding theories. In addition to the value of reaching an improved understanding of 3c4e halogen bonds from a theoretical perspective, the rapidly growing awareness of the wide synthetic applicability of electrophilic halogenating agents^{25,26,75–77} indicates the practical importance of the studies that we have reported above. Accordingly, fundamental insights into the 3c4e halogen bond are of critical importance to several fields, especially synthetic and medicinal chemistry.

Acknowledgements

The research leading to these results has received funding from the European Union Seventh Framework Programme (FP7/2007–2013) under grant agreement no. 259638, and from the Swedish Research Council (2012–3819). We thank the Swedish National Infrastructure for Computing (SNIC) for generous allotment of computing time. J. G. thanks the Royal Society for Arts and Sciences in Gothenburg and the Sigurd and Elsa Golje Memorial Foundation for financial support.

Notes and references

- 1 W. A. Noyes and A. C. Lyon, *J. Am. Chem. Soc.*, 1901, **23**, 460–463.
- 2 J. Stieglitz, *J. Am. Chem. Soc.*, 1904, **23**, 797–799.
- 3 I. Roberts and G. E. Kimball, *J. Am. Chem. Soc.*, 1937, **59**, 947–948.
- 4 G. A. Olah, *Halonium ions*, Wiley & Sons, New York, USA, 1975.
- 5 G. A. Olah, J. M. Bollinger and J. Brinich, *J. Am. Chem. Soc.*, 1968, **90**, 2587–2594.
- 6 B. K. Ohta, T. M. Scupp and T. J. Dudley, *J. Org. Chem.*, 2008, **73**, 7052–7059.
- 7 B. K. Ohta, R. E. Hough and J. W. Schubert, *Org. Lett.*, 2007, **9**, 2317–2320.
- 8 X. S. Bogle and D. A. Singleton, *J. Am. Chem. Soc.*, 2011, **133**, 17172–17175.
- 9 E. S. Stoyanov, I. V. Stoyanova, F. S. Tham and C. A. Reed, *J. Am. Chem. Soc.*, 2010, **132**, 4062–4063.
- 10 M. D. Struble, M. T. Scerba, M. Siegler and T. Lectka, *Science*, 2013, **340**, 57–60.
- 11 G. D. Brayer and M. N. G. James, *Acta Crystallogr., Sect. B: Struct. Crystallogr. Cryst. Chem.*, 1982, **38**, 654–657.
- 12 I. Haque and J. L. Wood, *J. Mol. Struct.*, 1968, **2**, 217–238.
- 13 A.-C. C. Carlsson, J. Gräfenstein, A. Budnjo, J. L. Laurila, J. Bergquist, A. Karim, R. Kleinmaier, U. Brath and M. Erdelyi, *J. Am. Chem. Soc.*, 2012, **134**, 5706–5715.
- 14 A.-C. C. Carlsson, M. Uhrbom, A. Karim, U. Brath, J. Gräfenstein and M. Erdelyi, *CrystEngComm*, 2013, **15**, 3087–3092.
- 15 R. D. Parra, *Comput. Theor. Chem.*, 2012, **998**, 183–192.
- 16 D. C. Georgiou, P. Butler, E. C. Browne, D. J. D. Wilson and J. L. Dutton, *Aust. J. Chem.*, 2013, **66**, 1179–1188.
- 17 M. Erdelyi, *Chem. Soc. Rev.*, 2012, **41**, 3547–3557.
- 18 G. R. Desiraju, P. S. Ho, L. Kloo, A. C. Legon, R. Marquardt, P. Metrangolo, P. Politzer, G. Resnati and K. Rissanen, *Pure Appl. Chem.*, 2013, **85**, 1711–1713.
- 19 R. W. Troff, T. Makela, F. Topic, A. Valkonen, K. Raatikainen and K. Rissanen, *Eur. J. Org. Chem.*, 2013, 1617–1637.
- 20 C. L. Perrin, P. Karri, C. Moore and A. L. Rheingold, *J. Am. Chem. Soc.*, 2012, **134**, 7766–7772.
- 21 J. Guo, P. M. Tolstoy, B. Koeppel, N. S. Golubev, G. S. Denisov, S. N. Smirnov and H. H. Limbach, *J. Phys. Chem. A*, 2012, **116**, 11180–11188.
- 22 C. L. Perrin, *Acc. Chem. Res.*, 2010, **43**, 1550–1557.
- 23 P. Metrangolo and G. Resnati, *Science*, 2008, **321**, 918–919.
- 24 P. Metrangolo, H. Neukirch, T. Pilati and G. Resnati, *Acc. Chem. Res.*, 2005, **38**, 386–395.
- 25 J. Barluenga, *Pure Appl. Chem.*, 1999, **71**, 431–436.
- 26 R. S. Brown, A. A. Neverov, C. T. Liu and C. I. Maxwell, *ACS Symp. Ser.*, 2007, **965**, 458–476.
- 27 M. N. Eberlin, T. Kotiaho, B. J. Shay, S. S. Yang and R. G. Cooks, *J. Am. Chem. Soc.*, 1994, **116**, 2457–2465.
- 28 S. S. Yang, O. Bortolini, A. Steinmetz and R. G. Cooks, *J. Mass Spectrom.*, 1995, **30**, 184–193.
- 29 J. R. Sabin, *J. Mol. Struct.*, 1972, **11**, 33–51.
- 30 P. Metrangolo, F. Meyer, T. Pilati, G. Resnati and G. Terraneo, *Angew. Chem., Int. Ed.*, 2008, **47**, 6114–6127.
- 31 R. Wilcken, M. O. Zimmermann, A. Lange, A. C. Joerger and F. M. Boeckler, *J. Med. Chem.*, 2013, **56**, 1363–1388.
- 32 T. M. Beale, M. G. Chudzinski, M. G. Sarwar and M. S. Taylor, *Chem. Soc. Rev.*, 2013, **42**, 1667–1680.
- 33 A. Caballero, N. G. White and P. D. Beer, *Angew. Chem., Int. Ed.*, 2011, **50**, 1845–1848.
- 34 S. M. Walter, F. Kniep, L. Rout, F. P. Schmidtchen, E. Herdtweck and S. M. Huber, *J. Am. Chem. Soc.*, 2012, **134**, 8507–8512.
- 35 A.-C. C. Carlsson, J. Gräfenstein, J. L. Laurila, J. Bergquist and M. Erdelyi, *Chem. Commun.*, 2012, **48**, 1458–1460.
- 36 M. Vanderpuy, *Tetrahedron Lett.*, 1987, **28**, 255–258.
- 37 T. Umemoto, K. Harasawa, G. Tomizawa, K. Kawada and K. Tomita, *J. Fluorine Chem.*, 1991, **53**, 369–377.
- 38 S. Castro-Fernández, I. R. Lahoz, A. L. Llamas-Saiz, J. L. Alonso-Gómez, M.-M. Cid and A. Navarro-Vázquez, *Org. Lett.*, 2014, **16**, 1136–1139.
- 39 A. J. Poss, M. Vanderpuy, D. Nalewajek, G. A. Shia, W. J. Wagner and R. L. Frenette, *J. Org. Chem.*, 1991, **56**, 5962–5964.
- 40 R. E. Banks, S. N. Mohialdinkhaffaf, G. S. Lal, I. Sharif and R. G. Syvret, *Chem. Commun.*, 1992, 595–596.
- 41 S. H. Vosko, L. Wilk and M. Nusair, *Can. J. Phys.*, 1980, **58**, 1200–1211.
- 42 A. D. Becke, *Phys. Rev. A*, 1988, **38**, 3098–3100.
- 43 A. D. Becke, *J. Chem. Phys.*, 1993, **98**, 5648–5652.
- 44 C. T. Lee, W. T. Yang and R. G. Parr, *Phys. Rev. B: Condens. Matter Mater. Phys.*, 1988, **37**, 785–789.
- 45 P. J. Stephens, F. J. Devlin, C. S. Ashvar, C. F. Chabalowski and M. J. Frisch, *Faraday Discuss.*, 1994, **99**, 103–119.
- 46 L. E. Roy, P. J. Hay and R. L. Martin, *J. Chem. Theory Comput.*, 2008, **4**, 1029–1031.
- 47 P. J. Hay and W. R. Wadt, *J. Chem. Phys.*, 1985, **82**, 270–283.
- 48 P. J. Hay and W. R. Wadt, *J. Chem. Phys.*, 1985, **82**, 299–310.
- 49 W. R. Wadt and P. J. Hay, *J. Chem. Phys.*, 1985, **82**, 284–298.
- 50 R. Krishnan, J. S. Binkley, R. Seeger and J. A. Pople, *J. Chem. Phys.*, 1980, **72**, 650–654.
- 51 A. D. Mclean and G. S. Chandler, *J. Chem. Phys.*, 1980, **72**, 5639–5648.
- 52 T. Clark, J. Chandrasekhar, G. W. Spitznagel and P. V. Schleyer, *J. Comput. Chem.*, 1983, **4**, 294–301.
- 53 M. Cossi, G. Scalmani, N. Rega and V. Barone, *J. Chem. Phys.*, 2002, **117**, 43–54.
- 54 B. Mennucci and J. Tomasi, *J. Chem. Phys.*, 1997, **106**, 5151–5158.
- 55 Y. Shao, L. F. Molnar, Y. Jung, J. Kusmann, C. Ochsenfeld, S. T. Brown, A. T. Gilbert, L. V. Slipchenko, S. V. Levchenko, D. P. O'Neill, R. A. DiStasio, Jr, R. C. Lochan, T. Wang, G. J. Beran, N. A. Besley, J. M. Herbert, C. Y. Lin, T. Van Voorhis, S. H. Chien, A. Sodt, R. P. Steele, V. A. Rassolov, P. E. Maslen, P. P. Korambath, R. D. Adamson, B. Austin, J. Baker, E. F. Byrd, H. Dachsel, R. J. Doerksen, A. Dreuw, B. D. Dunietz, A. D. Dutoi, T. R. Furlani, S. R. Gwaltney, A. Heyden, S. Hirata, C. P. Hsu, G. Kedziora, R. Z. Khalliulin, P. Klunzinger, A. M. Lee, M. S. Lee,

- W. Liang, I. Lotan, N. Nair, B. Peters, E. I. Proynov, P. A. Pieniazek, Y. M. Rhee, J. Ritchie, E. Rosta, C. D. Sherrill, A. C. Simmonett, J. E. Subotnik, H. L. Woodcock, 3rd, W. Zhang, A. T. Bell, A. K. Chakraborty, D. M. Chipman, F. J. Keil, A. Warshel, W. J. Hehre, H. F. Schaefer, 3rd, J. Kong, A. I. Krylov, P. M. Gill and M. Head-Gordon, *Phys. Chem. Chem. Phys.*, 2006, **8**, 3172–3191.
- 56 M. J. Frisch, G. W. Trucks, H. B. Schlegel, G. E. Scuseria, M. A. Robb, J. R. Cheeseman, G. Scalmani, V. Barone, B. Mennucci, G. A. Petersson, H. Nakatsuji, M. Caricato, X. Li, H. P. Hratchian, A. F. Izmaylov, J. Bloino, G. Zheng, J. L. Sonnenberg, M. Hada, M. Ehara, K. Toyota, R. Fukuda, J. Hasegawa, M. Ishida, T. Nakajima, Y. Honda, O. Kitao, H. Nakai, T. Vreven, J. A. Montgomery Jr, J. E. Peralta, F. Ogliaro, M. Bearpark, J. J. Heyd, E. Brothers, K. N. Kudin, V. N. Staroverov, R. Kobayashi, J. Normand, K. Raghavachari, A. Rendell, J. C. Burant, S. S. Iyengar, J. Tomasi, M. Cossi, N. Rega, N. J. Millam, M. Klene, J. E. Knox, J. B. Cross, V. Bakken, C. Adamo, J. Jaramillo, R. Gomperts, R. E. Stratmann, O. Yazyev, A. J. Austin, R. Cammi, C. Pomelli, J. W. Ochterski, R. L. Martin, K. Morokuma, V. G. Zakrzewski, G. A. Voth, P. Salvador, J. J. Dannenberg, S. Dapprich, A. D. Daniels, Ö. Farkas, J. B. Foresman, J. V. Ortiz, J. Cioslowski and D. J. Fox, *vol. Revision D.01*, Gaussian, Inc., Wallingford CT, 2009.
- 57 A. D. Becke, *J. Chem. Phys.*, 2003, **119**, 2972–2977.
- 58 J. Gräfenstein and D. Cremer, *Theor. Chem. Acc.*, 2009, **123**, 171–182.
- 59 C. Moller and M. S. Plesset, *Phys. Rev.*, 1934, **46**, 0618–0622.
- 60 Y. Zhao and D. G. Truhlar, *Theor. Chem. Acc.*, 2008, **120**, 215–241.
- 61 S. Grimme, J. Antony, S. Ehrlich and H. Krieg, *J. Chem. Phys.*, 2010, **132**, 154104.
- 62 Y. Lu, H. Li, X. Zhu, W. Zhu and H. Liu, *J. Phys. Chem. A*, 2011, **115**, 4467–4475.
- 63 A. Bondi, *J. Phys. Chem.*, 1964, **68**, 441–451.
- 64 W. Z. Wang, N. B. Wong, W. X. Zheng and A. M. Tian, *J. Phys. Chem. A*, 2004, **108**, 1799–1805.
- 65 L. P. Wolters and F. M. Bickelhaupt, *ChemistryOpen*, 2012, **1**, 96–105.
- 66 C. L. Perrin and K. D. Bruke, *J. Am. Chem. Soc.*, 2014, **136**, 4355–4362.
- 67 A. E. Reed, R. B. Weinstock and F. Weinhold, *J. Chem. Phys.*, 1985, **83**, 735–746.
- 68 C. L. Perrin, *Pure Appl. Chem.*, 2009, **91**, 571–593.
- 69 A. E. Reed and F. Weinhold, *J. Chem. Phys.*, 1983, **78**, 4066–4073.
- 70 P. Metrangolo, J. S. Murray, T. Pilati, P. Politzer, G. Resnati and G. Terraneo, *Cryst. Growth Des.*, 2011, **11**, 4238–4246.
- 71 P. Metrangolo, J. S. Murray, T. Pilati, P. Politzer, G. Resnati and G. Terraneo, *CrystEngComm*, 2011, **13**, 6593–6596.
- 72 S. Shaik, H. B. Schlegel and S. Wolfe, *Theoretical aspects of physical organic chemistry: the SN2 mechanism*, Wiley, New York, 1992.
- 73 R. A. Fireston, *J. Org. Chem.*, 1971, **36**, 702–711.
- 74 G. A. Landrum, N. Goldberg and R. Hoffmann, *J. Chem. Soc., Dalton Trans.*, 1997, 3605–3613.
- 75 T. Umemoto, S. Fukami, G. Tomizawa, K. Harasawa, K. Kawada and K. Tomita, *J. Am. Chem. Soc.*, 1990, **112**, 8563–8575.
- 76 G. S. Lal, G. P. Pez and R. G. Syvret, *Chem. Rev.*, 1996, **96**, 1737–1755.
- 77 G. G. Furin and A. A. Fainzilberg, *Usp. Khim.*, 1999, **68**, 725–759.